



HAL
open science

Push–Pull Fluorescent Dyes with Trifluoroacetyl Acceptor for High-Fidelity Sensing of Polarity and Heterogeneity of Lipid Droplets

Nathan Aknine, Andrey Klymchenko

► **To cite this version:**

Nathan Aknine, Andrey Klymchenko. Push–Pull Fluorescent Dyes with Trifluoroacetyl Acceptor for High-Fidelity Sensing of Polarity and Heterogeneity of Lipid Droplets. *Analytical Chemistry*, 2024, 96 (32), pp.13242-13251. 10.1021/acs.analchem.4c02322 . hal-04684663

HAL Id: hal-04684663

<https://hal.science/hal-04684663v1>

Submitted on 3 Sep 2024

HAL is a multi-disciplinary open access archive for the deposit and dissemination of scientific research documents, whether they are published or not. The documents may come from teaching and research institutions in France or abroad, or from public or private research centers.

L'archive ouverte pluridisciplinaire **HAL**, est destinée au dépôt et à la diffusion de documents scientifiques de niveau recherche, publiés ou non, émanant des établissements d'enseignement et de recherche français ou étrangers, des laboratoires publics ou privés.

Copyright

Push-pull fluorescent dyes with trifluoroacetyl acceptor for high-fidelity sensing of polarity and heterogeneity of lipid droplets

Nathan Aknine and Andrey S. Klymchenko*

Laboratoire de Bioimagerie et Pathologies, UMR 7021 CNRS, ITI SysChem, Faculté de Pharmacie, Université de Strasbourg, 67401 Illkirch, France. E-mail: andrey.klymchenko@unistra.fr

Abstract

Imaging and sensing of lipid droplets (LDs) attracted significant attention, due to growing evidences for their important role in cell life. Solvatochromic dyes are promising tools to probe LDs local polarity, but this analysis is biased by their non-negligible emission from intracellular membranes and capacity to emit from both the apolar core and polar interface of LDs. Here, we developed two push-pull solvatochromic dyes based on naphthalene and fluorene core bearing an exceptionally strong electron acceptor, trifluoroacetyl group. The latter was found to boost the optical properties of the dyes by shifting their absorption and emission to the red, increasing their extinction coefficient, photostability, and sensitivity to solvent polarity (solvatochromism). In contrast to classical solvatochromic dyes, such as parent aldehydes and reference Nile Red, the new dyes exhibited strong fluorescence quenching by mM water concentrations in organic solvents. In live cells, the trifluoroacetyl dyes exhibited high specificity to LDs, whereas the parent aldehydes and Nile Red showed detectable background from intracellular membranes. Experiments in model lipid membranes and nanoemulsions droplets confirmed high selectivity of new probes to LDs in contrast to classical solvatochromic dyes. Moreover, the new probes were found to be selective to LDs oil core, where they can sense lipid unsaturation and chain length. Their ratiometric imaging in cells revealed strong heterogeneity in polarity within LDs, which covered the range of polarities of unsaturated triglyceride oils, whereas Nile Red failed to properly estimate local polarity of LDs. Finally, the probes revealed that LDs core polarity can be altered by fatty acid diets, which correlated with their chain length and unsaturation.

Introduction

Fluorescent solvatochromic dyes gained significant attention in the last decades both in terms of their unique photophysics and the multitude of their applications in biology.¹ These are smart “chameleon” dyes that shift their emission maximum as a function of solvent polarity.² The most popular are push-pull dyes, which undergo excited state charge transfer (ICT) and increase their dipole moment in the excited state.¹ The latter leads to positive fluorescence solvatochromism, so that more polar solvents shift their emission bands towards longer wavelengths. These dyes conquer the field of chemical biology and biophysics, allowing detection of lipid organization of lipid membranes,³⁻⁷ sensing biomolecular interactions,⁸⁻⁹ super-resolution imaging,¹⁰⁻¹² etc. Particular exciting examples are recent applications of these probes for sensing local polarity in lipid structures of organelles,^{7,13-14}

including lipid droplets.¹⁵⁻²¹ The latter are membrane-less compartments characterized by highly apolar oil core and shell built from proteins, phospholipids, and fatty acids.²²⁻²⁴ They raised particular interest recently, because the status of lipid droplets may reflect a number of pathologies, such as tumorigenesis, oxidative stress, and deregulations in lipid metabolism (e.g. fatty liver disease, atherosclerosis, lipodystrophy), etc.²⁵⁻²⁸ A tremendous effort has been done in the last decade to develop useful fluorescent molecular markers for LDs.¹⁹ However, the design and use of solvatochromic dyes for LDs is still not sufficiently explored. They provide important information about local polarity of LDs as well as their heterogeneity,^{16,20} which could be directly related to the variation in their lipid composition, age, and functional state. The problem is that the vast majority of solvatochromic dyes exhibit rather strong fluorescence in lipid membranes.¹ Therefore, Nile Red and other push-pull dyes present non-negligible emission from lipid membranes,^{11,20-21,29} which create a fluorescence background, that largely complicates analysis of local polarity in lipid droplets. Moreover, these dyes emit from both core and shell of LDs, so that the local polarity is ill-defined. Therefore, highly selective targeting and sensing of LDs would require specific targeting of their oil core, avoiding parasite fluorescence from the shell and intracellular membranes. This could be realized by implementation of fluorogenic character into solvatochromic dyes, which could be effectively quenched at interfaces of LDs and biomembranes.

The typical push-pull dye is composed of an electron donor (usually dialkylamino group) and an electron acceptor. A number of electron acceptors have been used so far, which include aldehyde and ketone, carboxylate, sulfonate as well as some heterocycles, like pyridine, pyridinium, rhodanine, etc.¹ The increase in the strength of electron donor and acceptor groups and the conjugation length usually leads to higher charge transfer character (transition dipole moment) and thus higher solvatochromism, i.e. sensitivity to solvent polarity. An additional interesting factor, stronger charge transfer also leads to the increase in the fluorescence quenching of the dyes in highly polar environments, usually by twisted intramolecular charge transfer (TICT) mechanism,³⁰ which render them fluorogenic in apolar media.¹ Therefore, typical solvatochromic dyes are highly emissive in both lipid membranes from lipid droplets, owing to their rather apolar environment.³ To achieve higher selectivity for LDs, one should implement a quenching mechanism, which could operate in lipid membranes, but not in the highly apolar core of LDs. We considered using trifluoroacetyl group as an electron acceptor. On the other hand, it is one of the strongest electron-withdrawing groups with Hammett acceptor properties ($\sigma_p = 0.80$) much larger than the aldehyde ($\sigma_p = 0.42$).³¹ It could enhance the solvatochromism of the dyes together with higher quenching in polar environments and water molecules. Second, highly electron-deficient carbonyl of trifluoroacetyl could be attacked by nucleophiles, including water, which could lead to additional quenching by water. However, trifluoroacetyl group was rarely used in the design of solvatochromic dyes, while the major focus of these studies was oriented to design chemosensors for amines and alcohols due to their addition of the carbonyl group.³²⁻³⁵ A more recent report proposed this group for implementing water sensing moiety for sensing water and super-resolution imaging application.³⁶⁻³⁷ Overall, none of the reports on trifluoroacetylated dyes proposed application for sensing and imaging of LDs.

In the present work, we developed two push-pull dyes bearing trifluoroacetyl acceptor group, which showed excellent specificity to the LDs vs intracellular membranes. We found that the trifluoroacetyl group boosted the optical properties of the dyes by shifting their absorption and emission to the red, increasing their extinction coefficient and photostability. Importantly, in contrast to their parent aldehydes, they exhibited strong fluorescence quenching by water at mM concentrations in organic

solvents. In cells, the new trifluoroacetyl exhibited high specificity to LDs, while Nile Red exhibited a detectable background from intracellular membranes. Experiments in model systems showed that the new dyes are effectively quenched in lipid membranes being highly emissive in lipid droplets, while Nile Red and patent aldehydes cannot distinguish them well. We found that the new dyes are highly selective to LD oil core, where they can sense lipid unsaturation and chain length. The ratiometric imaging of the new dyes in cells revealed strong heterogeneity in polarity within LDs. The probes evidenced the effect of fatty acid diets on LDs, which provides a clear connection between local polarity of the LD core and its lipid composition.

Results and discussion

The push-pull dyes ProCF3 and FrCF3 were designed based on naphthalene and fluorene aromatic cores, respectively (Figure 1A). Previously, these aromatic cores were used to design Prodan³⁸ and FR0,³⁹ which can be considered as classical push-pull dyes with remarkably high solvatochromism.¹ Here, we kept their dialkylamino group as a donor, but replaced their carbonyl group with a much stronger electron acceptor trifluoroacetyl group (Figure 1A). We hypothesized that the use of this strong electron acceptor could improve the optical properties of the dyes and provide their efficient quenching in water. The latter could make these dyes highly emissive in the hydrophobic core of lipid droplets, but quenched in hydrated lipid membranes, which would allow selective sensing of local polarity in the LDs core (Figure 1B). Introduction of the trifluoroacetyl group required synthesis of appropriate aryl bromides **1** and **4** (Scheme S1). They were further converted into the target trifluoroacetyl derivatives ProCF3 (**2**) and FrCF3 (**5**) by reaction with n-butyl lithium and N-Methyl-N-methoxytrifluoroacetamide through Weinreb ketone synthesis (Figure 1A). The obtained products were purified by column chromatography and identified by NMR and mass spectrometry. They were further studied in comparison to their close analogues bearing aldehyde instead of trifluoroacetyl group: ProCHO (**3**) and FR0 (or FrCHO).³⁹ ProCHO was obtained from the aryl bromide **1** with n-butyl lithium and DMF (see supporting information). The identity and purity of all new compounds were confirmed by mass and NMR spectrometry (the images of NMR spectra are shown in Figures S1-S10).

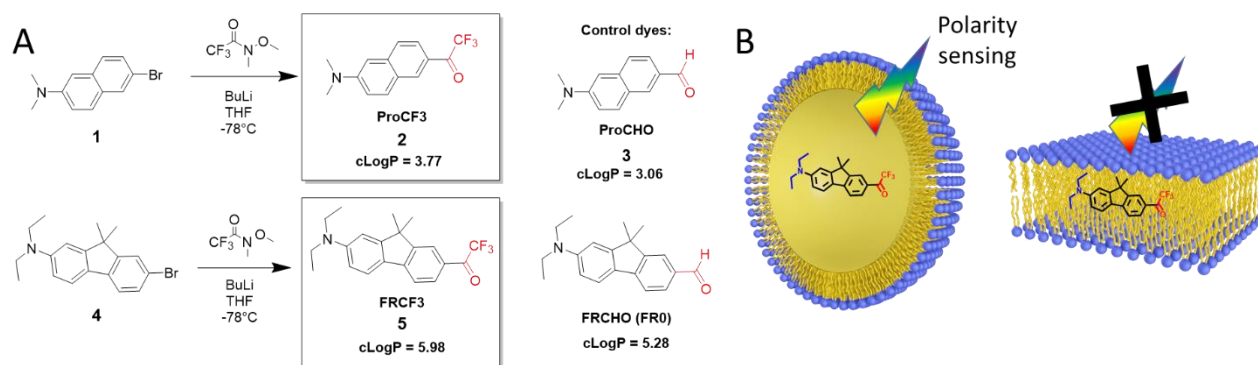


Figure 1. (A) Push-pull dyes with trifluoroacetyl acceptor and their parent (control) dyes. Electron donor is shown in blue, while electron acceptor is in red. Synthetic scheme for the naphthalene and fluorene-based dyes. Calculated logP values (cLogP) are shown for studied dyes. (B) Hypothesis of the work: efficient emission of new dyes in the core of LDs and poor emission in the lipid membranes, caused by fluorescence quenching.

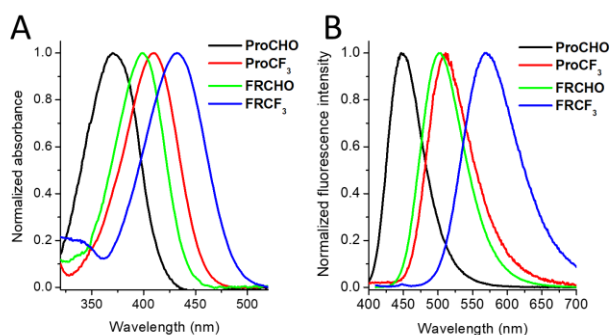


Figure 2. Normalized absorption (A) and fluorescence (B) spectra of trifluoroacetyl-based dyes vs their aldehyde-based analogues in dichloromethane.

Absorption and fluorescence spectra of the dyes were studied in organic solvents (Figure 2, S11 and S12, Table S1). It was found that both new dyes exhibit single absorption bands, strongly shifted to the red compared with their aldehyde analogues (ProCHO and FR0): ~40 and ~30 nm for ProCF3 (**2**) and FrCF3 (**5**), respectively. This result indicates that much stronger electron acceptor properties of trifluoroacetyl group greatly enhance the push-pull characteristics and charge transfer character of the dyes, which decreases the transition energy. Importantly, trifluoroacetyl makes both dyes absorb in the visible range, which is useful for their applications with a common violet laser, such as 405 nm. Similar redshifts were also observed in the emission spectra (Figure 2 and Table S1), while the Stokes shifts increased mainly for FrCF3 vs FR0.

Next, we studied the effect of solvent polarity on the optical properties of the dyes. The absorption maxima showed relatively poor dependence on the solvent polarity (Table S1), whereas fluorescence exhibited pronounced red shifts with an increase in the solvent polarity (Figure 3A,B). A clear correlation was found between emission maximum and polarity index $E_T(30)$ (Figure 3C), which is an empirical polarity index.² Moreover, trifluoroacetyl dramatically enhanced the solvatochromism of naphthalene-based dye, as it can be seen from the much higher slope of the polarity plot for ProCF3 vs ProCHO. It was even slightly higher than that of FR0, known as one of the most solvatochromic dyes to date. Here, higher solvatochromism was achieved for the even smaller dye, which makes it attractive for biological applications where compact dyes are crucial. Trifluoroacetyl also enhanced solvatochromism of FrCF3 vs FR0, although the effect was less pronounced. Another important observation is variation of the fluorescence intensity (Figure S2) and quantum yield (Table S1) of the new dyes as a function of solvent polarity. At low and medium polar solvents, the QY values were high, similarly to their aldehyde analogues, whereas in highly polar solvents their QY dropped dramatically, so that their values were ~10-fold lower. The effect was particularly dramatic for FrCF3, which showed almost negligible emission in the polar protic solvents methanol and water. One should also notice that in protic solvents methanol and water, and in aprotic DMSO, ProCF3 showed a new blue-shifted emission band (Figure S2). Absorption spectra in these solvents showed enhancement of the blue-shifted band around 300 nm (Figure S1). We hypothesize that this phenomenon is probably linked to the addition of the protic solvent and DMSO to the highly electrophilic carbon of trifluoroacetyl group, which is known for this class of compounds. The latter leads to the loss of conjugation with the aryl unit and thus strong blue shifts in the absorption and emission bands. Similar phenomena in absorption were observed for FrCF3, whereas its emission was strongly quenched in these solvents.

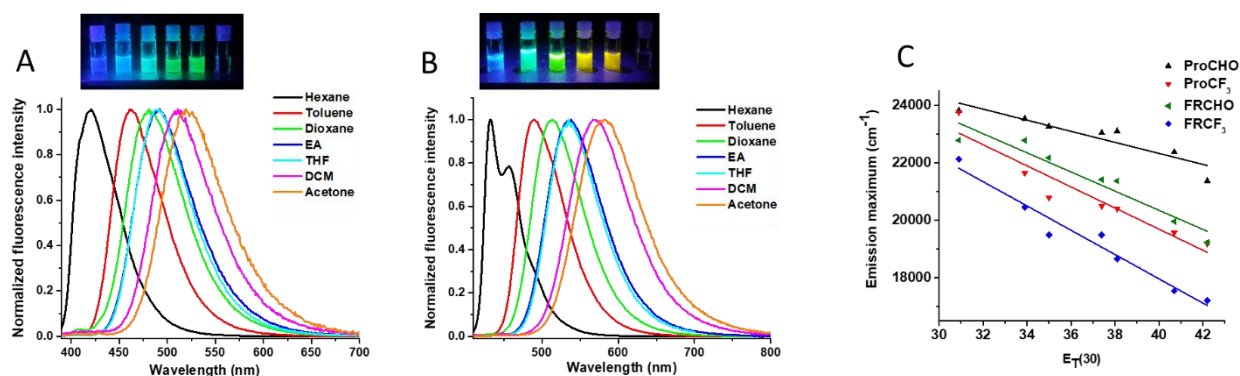


Figure 3. Normalized fluorescence spectra of ProCF₃ (A) and FrCF₃ (B) in aprotic solvents of different polarity. (C) Dependence of emission maximum on polarity index $E_T(30)$.

To further study the effect of solvent polarity on the emission of the dyes, we performed titration of these dyes in apolar 1,4-dioxane with water (Figures 4 and S13). As expected, the emission of the new dyes shifted to the red with an increase in water concentration, which was accompanied by a dramatic drop in the fluorescence intensity. In contrast, the parent aldehyde analogues ProCHO (**3**) and FR0 displayed the redshift without a significant drop in the fluorescence intensity (Figures 4 and S13). Thus, the experiments in neat solvents and solvent mixtures suggest that trifluoroacetyl group provided the push-pull dyes with fluorogenic character, showing efficient quenching in polar solvents, in addition to classical solvatochromism. Titration with deuterated water (Figure S14), commonly used to evaluate the role of the H-bonding in fluorescence quenching,⁴⁰ also revealed strong quenching, even though the intensity values with D₂O were slightly higher compared to water (Figure S14). Thus, H-bonding may contribute to some extent to the quenching of these dyes by water, but the major role is played by the dipole-dipole interactions, which favor formation of strongly quenched TICT states³⁰ of the dyes (see supporting information for details).

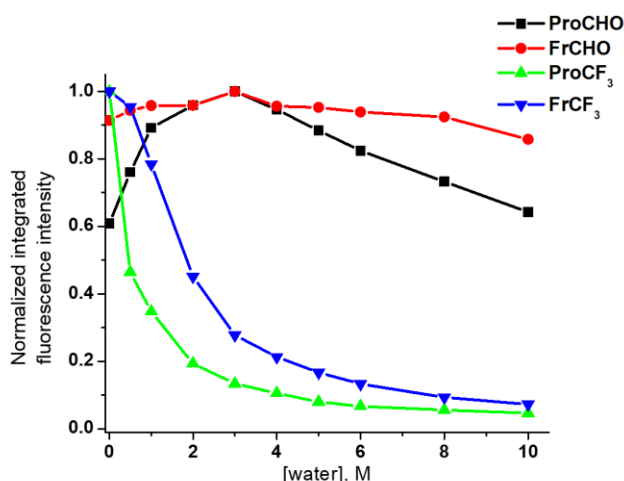


Figure 4. The integral fluorescence intensity of four studies dyes vs water concentration in 1,4-dioxane.

Finally, we studied the photostability of the new dyes in organic solvent THF in comparison to their parent analogues. The continuous irradiation of ProCF₃ (**2**) and FrCF₃ (**5**) produced minimal effects

on the fluorescence intensity of the dyes over time, whereas a significant drop in the fluorescence intensity was observed for the ProCHO and FR0 (Figure S15). The most striking was the behavior of FrCF3, which did not show any sign of photo-degradation in our experimental conditions. We could speculate that in this rather apolar environment the aldehyde derivatives, the excited S1 state could be prone to the intersystem crossing, known for Prodan derivative, which would lead to the triplet state and further decomposition through photo-oxidation.⁴¹ This is probably not the case because of the much lower energy of the S1 state of ProCF3 and especially FrCF3. Moreover, trifluoroacetyl group could additionally decrease the chances of photo-oxidation due to its strong electron acceptor properties.

Overall, trifluoroacetyl group produced several dramatic effects on the optical properties of push-pull dyes: (1) it shifted absorption and emission maxima to the red by >30 nm; (2) it improved solvatochromism, especially for smaller naphthalene analogue; (3) it rendered dyes with fluorogenic character and (4) it dramatically enhanced their photostability.

The new dyes are expected to perform best in highly apolar media, while they are expected to be strongly quenched in aqueous media. This would be particularly attractive for imaging LDs, which are the most apolar compartments of the cells due to the presence of the hydrophobic oil core. Therefore, we incubated the new dyes in live cells (U87) and further imaged them using fluorescence confocal microscopy in the presence of reference LDs marker Nile Red. To detect corresponding dyes, we recorded the nearly entire spectral range of each dye, which could provide us an idea about labelling specificity of LDs. The obtained images showed bright dots inside the cells, which co-localized well with the emission of Nile Red (Figure 5), with Pearson's coefficient of 0.78 and 0.70 for ProCF3 and FrCF3, respectively. These values were not so high, probably because Nile Red exhibited a significant background inside the cells (Figure 5), which corresponded to the non-specific staining by Nile Red of intracellular membranes. When Nile Red was recorded at the short-wavelength part of its spectrum, this background was much lower, because red-shifted emission of intracellular membranes was excluded (Figure S16). As a result, the Pearson's coefficients with ProCF3 and FrCF3 (also recorded at the short-wavelength part of their spectrum) were much higher: 0.90 and 0.96, respectively. In contrast, ProCF3 and FrCF3 dyes did not show any sign of co-localization with mitochondria marker MitoTracker Deep Red and lysosome marker LysoTracker Deep Red (Figure S17), showing low values of Pearson's coefficients (0.3-0.4). We can conclude that both new dyes target well LDs and their fluorogenic character enables imaging LDs with a much higher signal-to-background ratio compared to the reference dye Nile Red. Parent dyes ProCHO and FR0 were also tested in cells, where the former showed practically no preference for LDs, while the latter displayed some selective emission from LDs (Figure S18), similar to Nile Red.

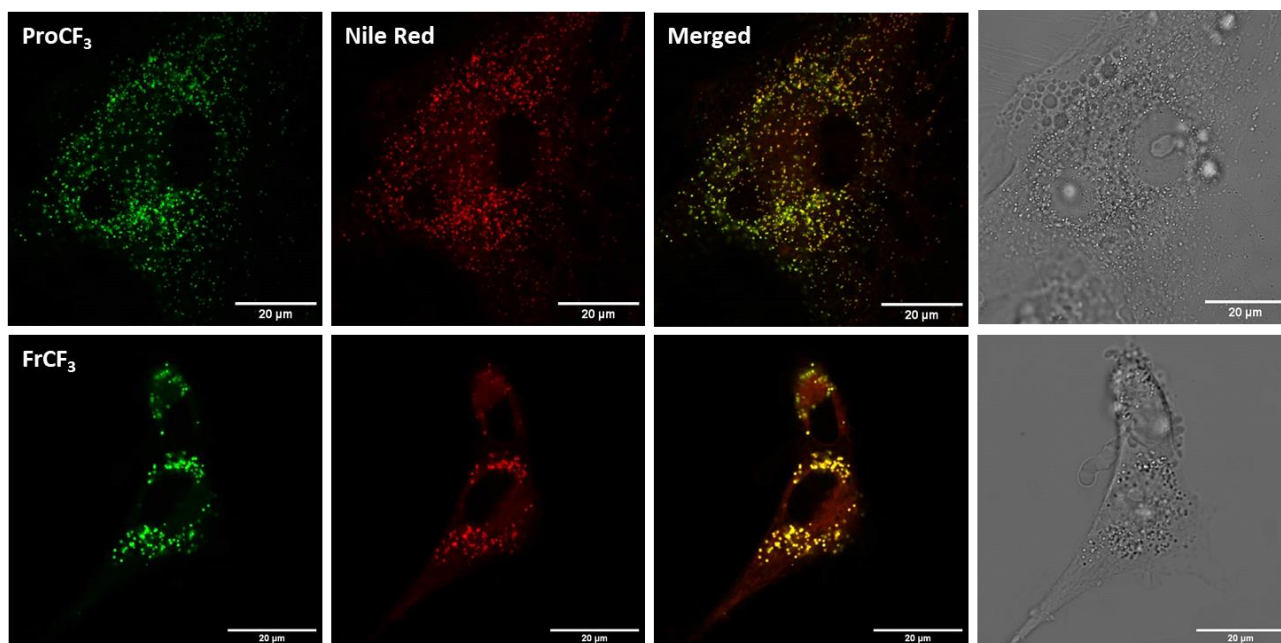


Figure 5. Fluorescence imaging of U87 cells labelled with ProCF3 and FrCF3 in comparison to Nile Red. Upper left panel: ProCF3. Lower left panel: FrCF3. Panels in red: Nile Red. Merged images and transmission images (right panels) are also shown. The excitation and emission wavelengths were the following: ProCF3: $\lambda_{\text{excitation}} = 405 \text{ nm}$; $\lambda_{\text{excitation}} = 420\text{-}520 \text{ nm}$; FrCF3: $\lambda_{\text{excitation}} = 405 \text{ nm}$; $\lambda_{\text{emission}} = 450\text{-}550 \text{ nm}$; Nile Red: $\lambda_{\text{excitation}} = 488 \text{ nm}$; $\lambda_{\text{emission}} = 600\text{-}700 \text{ nm}$ Colocalization Pearson's coefficients with Nile Red are 0.78 and 0.70 for ProCF3 and FrCF3, respectively. Dye concentrations: 200 nM for ProCF3 and FrCF3 and 50 nM for Nile Red, respectively. Scale bar: 20 μm .

To understand better the reason for high specificity of ProCF3 and FrCF3 to LDs, we estimated logP of these dyes (cLogP, Figure 1), which reflects the oil-water partition coefficient, important factor for targeting of dyes to LDs.⁴² For ProCF3 and FrCF3, cLogP values are 3.77 and 5.98, respectively, being close to that of Nile Red 4.62. These values are only slightly higher than those for corresponding aldehydes: 3.06 and 5.28 for ProCHO and FR0, respectively. The relatively high values of cLogP are a favorable factor for LDs targeting, but they cannot be the only explanation for the improved specificity of ProCF3 and FrCF3 compared to Nile Red and the parent aldehydes. We expect that the high specificity of ProCF3 and FrCF3 to LDs is mainly related to the strong quenching of the dyes in polar media, especially water. Moreover, it may indicate that these dyes do not light up in biological membranes, in contrast to Nile Red and the vast majority of solvatochromic dyes developed to date. To further understand this phenomenon, we compared the fluorescence intensity of the new dyes, their aldehyde analogues, and Nile Red in two model systems. First, we tested dyes in large unilamellar vesicles (LUVs) of 1,2-dioleoyl-sn-glycero-3-phosphocholine (DOPC) lipid, which are a close model of biomembranes. Nile Red and control aldehyde analogues ProCHO and FrCHO, showed strong emission in lipid membranes compared to the buffer, which confirmed a typical behavior of solvatochromic dyes, shielded from bulk water in lipid membranes (Figure 6A).¹ In sharp contrast, ProCF3 and FrCF3 in DOPC vesicles showed poor emission close to buffer, indicating that the dyes remain quenched in lipid membranes probably because of naturally present hydration water.⁴³⁻⁴⁵ This data corroborates with strong quenching of these dyes with the addition of water to 1,4-dioxane (Figure 4). Second, we tested our dyes in lipid nanoemulsions (NEs) composed of oil

core and surfactant shell, which constitute a close model of LDs.⁴⁶⁻⁴⁷ Again, the addition of Nile Red and control aldehydes to NEs resulted in strong fluorescence light-up (Figure 6A), owing to the apolar lipid environment of LDs. However, the fluorescence intensity in NEs was similar to that in LUVs, so Nile Red cannot distinguish well lipid droplets from lipid membrane. The latter explains the observed significant background for Nile Red in cells and the need to use the short-wavelength part of the emission spectrum (Figure S16), where the blue-shifted signal from LDs could be better distinguished from lipid membranes (see NEs vs LUVs, Figure S19). On the other hand, ProCF3 and FrCF3 showed strong fluorescence light-up in NEs compared to lipid membranes or buffer, indicating that they can clearly distinguish LDs from lipid membranes (Figure 6A and S19).

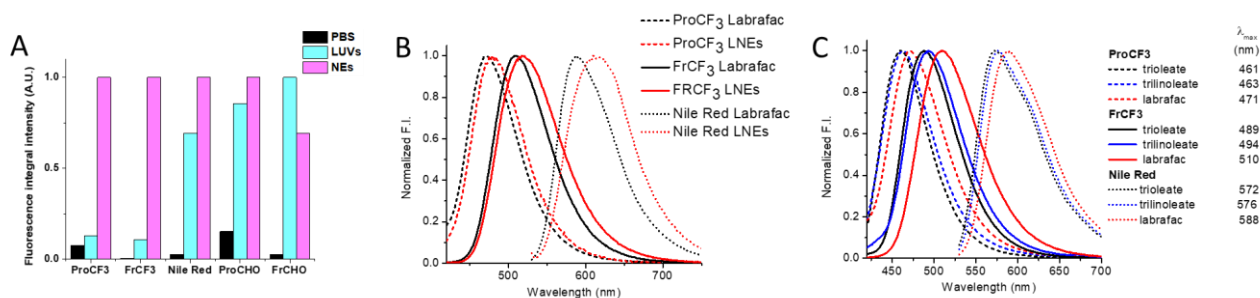


Figure 6. Specificity of ProCF3, FrCF3, and Nile Red to lipid droplets and sensitivity to the oil composition. (A) Integral fluorescence intensity of the three dyes at 2 μ M in PBS buffer, LUVs and NEs. (B) Spectral differences between NEs and neat Labrafac, constituting NEs oil core. (C) Spectral sensitivity of the three dyes in three oils of different fatty acid chain lengths and unsaturation levels.

Importantly, the emission maximum of ProCF3 and FrCF3 in NEs was close to that in the neat oil (Labrafac) used for the NEs formulation (Figure 6B). This indicates that when bound to NEs, the emission of these dyes originates from the droplet core, corresponding to the used oil. In case of Nile Red, the emission in NEs was significantly red-shifted compared to the oil Labrafac and the band appeared broader, indicating that this dye probably emits from both the droplet core and the interface. Similar effects were observed for model aldehydes ProCHO and FrCHO (Figure S20). Thus, classical solvatochromic dyes, which are not strongly quenched by water, exhibit strong emission at the interfaces of lipid membranes and lipid droplets and thus cannot distinguish them well. Moreover, they emit non-specifically from both the core and shell of LDs, which complicates data analysis. In contrast, ProCF3 and FrCF3 dyes are quenched by water at the interfaces of lipid membranes and LDs and emit predominantly in the oil core. This implies that they could be used for highly specific sensing of polarity in the core of LDs without adverse effects of their interface or intracellular membranes.

To understand better the sensitivity profile of the new probes, we studied their fluorescence spectra in three triglyceride oils: Labrafac, which is a mixture of saturated medium chain triglycerides (C8 and C10); (2) glyceryl trioleate having single unsaturation per fatty acid and (3) glyceryl trilinoleate, having double unsaturation per fatty acid. We found that the emission of new dyes and Nile Red in Labrafac was clearly red-shifted compared to the other two oils, which suggests that triglycerides with shorter fatty acid chains are characterized by higher polarity (Figure 6C). Moreover, for all studied dyes, the emission maximum in glyceryl trilinoleate was red-shifted compared to glyceryl trioleate (Figure 6C), suggesting that the increase in the unsaturation by one additional double bond

is detected by the dyes as an increase in the local polarity. The effect of unsaturation was clearly the largest in the case of FrCF3, probably because of its largest solvatochromism in the studied series of dyes.

Taking advantage of this particular sensitivity profile, we studied the polarity of LDs core by splitting the emission band of the dyes into the short-wavelength (SW) and long-wavelength (LW) channels. The SW channel corresponded to an emission window of 435-465 and 450-480 nm for ProCF3 and FrCF3, respectively, while the LW channel corresponded to 475-505 and 490-520 nm spectral window, respectively. The approach allows the detection of even slight changes in the local polarity observed in the lipid structures using solvatochromic probes.^{1,4} In cells, the lipid droplets appeared in different pseudo-colors ranging from blue to orange, revealing remarkable heterogeneity within droplets (Figure 7A). To interpret these data, we studied the calibration of the LW/SW ratio in the three model oils (Figure 7B). Importantly, the LW/SW ratio of the emission channels showed a clear increase in the following order: glyceryl trioleate < glyceryl trilinoleate << Labrafac (Figure 7C), which reflects the redshifts in the same order according to our spectroscopy studies (Figure 6C). It was found that the color variations within LDs were within the range observed in the three oils (Figure 7C). The blue droplets corresponded in polarity to glyceryl trioleate, the green ones – were closer to glyceryl trilinoleate, whereas orange ones were between glyceryl trilinoleate and Labrafac. Nevertheless, the observed polarity of LDs was much lower than that observed of oil Labrafac. The latter composed of unusually short fatty acid chains is clearly too polar to model natural LDs composed of natural fats. Similar effects were observed on ProCF3, although the effects were weaker due to lower solvatochromism (Figure S21). We performed a similar analysis for Nile Red. In sharp contrast, the LW/SW ratio of LDs obtained with Nile Red was much higher than that of glyceryl trioleate and glyceryl trilinoleate and it showed a second broad band with even higher polarity (Figure S22). The distribution of the LW/SW ratio values was close to that observed in the most polar Labrafac, indicating that the local polarity of LDs is overestimated by Nile Red, in contrast to the new probes. These results showed that the data of Nile Red were strongly contaminated by the signal recorded from the highly polar and hydrated interface of LDs and intracellular membranes. Close examination of the ratiometric image of the cells also showed heterogeneity of LDs (Figure S22), however, it could be clearly seen that the pseudo-colors for some LDs (green and orange) were out of range observed in model oils, reflecting much higher local polarity compared the most polar Labrafac. These green and orange dots were co-localized with a strong background from the intracellular membranes (white with LW/SW ratio >1), which are expected to present much higher local polarity. Thus, the heterogeneity of LDs reported by Nile Red is an artefact generated by the strong contribution of intracellular membranes. We expect that it could be a generic problem of classical solvatochromic dyes, whereas the artifact produced by these membranes is negligible for our new probes, because of their strong quenching by water.

These data provide direct evidence of the unique capacity of the new probes to sense directly the polarity of the oil core of LDs. They show that the LDs core polarity matches well natural oils, between glyceryl trioleate and glyceryl trilinoleate. Therefore, the variation of polarity in these LDs could reflect change in the oil composition of these droplets, which could depend on the level of maturation of these droplets.

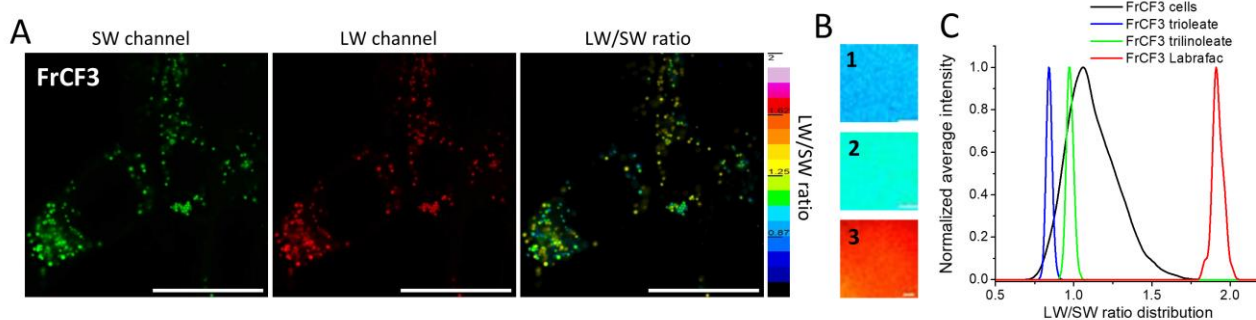


Figure 7. (A) Two-color ratiometric confocal imaging of U87 cells labelled with FrCF3 dye. Scale bars: 20 μm . (B) Ratiometric images of FrCF3 dye in three oils (1 – glyceryl trioleate; 2 – glyceryl trilinoleate and 3 – Labrafac), were recorded at the same conditions as for cells. Excitation: 405 nm. Emission windows are 450–480 nm and 490–520 nm for short-wavelength (SW) and long-wavelength (LW) channels, respectively. Dye concentration is 200 nM. Distribution of the LW/SW intensity ratio for cells in comparison to model oils, recorded under the same microscope. (C). Distribution of the LW/SW intensity ratio for cells in comparison to model oils, recorded under the same microscope.

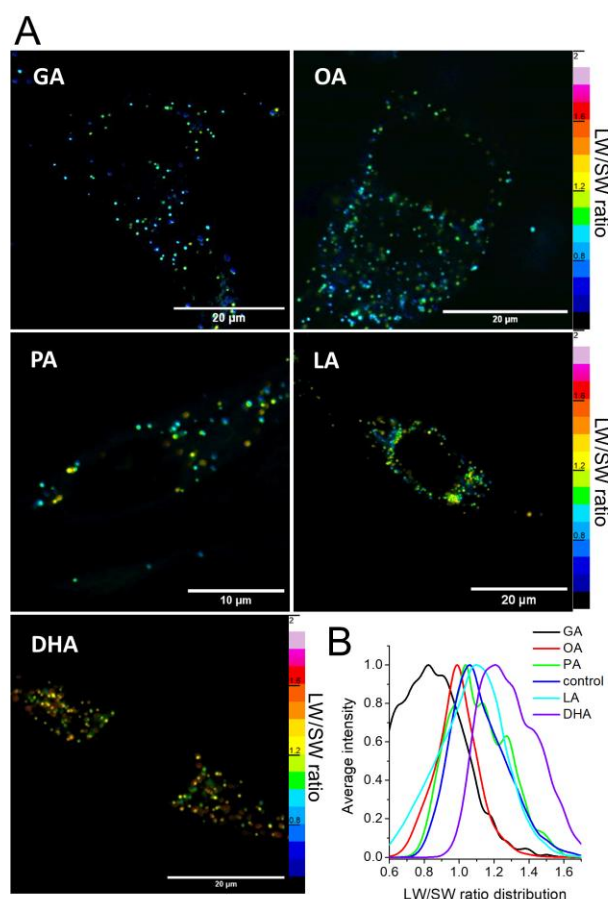


Figure 8. Effect of fatty acid diets on the two-color response of FrCF3 probe in LDs. (A) Confocal ratiometric imaging of U87 cells, labelled with FrCF3, after 24h fatty acids diet. Excitation wavelength: 405 nm. Emission wavelengths: are 450-480 and 490-520 nm for SW and LW channels, respectively. The cells were incubated for 24 h at 37°C with fatty acids at the following concentrations: 100 μM for gondoic acid (GA), 200 μM for oleic acid (OA) and palmitic acid (PA),

150 μM for linoleic acid (LA) and 20 μM for docosahexaenoic acid (DHA). Dye concentration is 200 nM. (B) Distribution of the LW/SW intensity ratio for cells after different fatty acid diets.

Finally, we took advantage of the strong solvatochromism of these probes to study how the polarity of lipid droplets can be affected by different lipid diets. For this purpose, we pre-incubated the cells in the presence of fatty acids with varied chain length and unsaturation and known to impact the activity of LDs: saturated palmitic acid (PA),⁴⁸ monounsaturated oleic acid (OA),⁴⁹⁻⁵⁰ diunsaturated linoleic acid (LA),⁵¹ polyunsaturated docosahexaenoic acid (DHA)⁵¹ and long-chain monounsaturated 11-eicosenoic acid (gondoic acid, GA).⁵² One can notice that for FrCF3, the fatty acid diets impacted the distribution of their LW/SW intensity ratio (Figure 8, S23). The LW/SW ratio increased in the following order $\text{GA} \ll \text{OA} \sim \text{PA} < \text{control} < \text{LA} \ll \text{DHA}$. Similar trends were observed for ProCF3 (Figure S24), although the effects were weaker due to the weaker solvatochromism of this dye. This trend, observed for both probes correlated well with the structure of fatty acids. First, the diet with PA and OA produced some decrease in the polarity, probably because it increased the content in saturated (PA) and long-chain monounsaturated (OA) fatty acids. Remarkably, very long-chain monounsaturated fatty acid (GA) produced a dramatic decrease in the LDs polarity, clearly because longer chain fatty acids are less polar molecules (Figure 8). In sharp contrast, polyunsaturated long-chain fatty acid DHA produced a strong increase in the LDs polarity compared to the control (Figure 8). Thus, higher levels of unsaturation, despite the long chain, produced an increase in the LDs polarity, clearly because unsaturated hydrocarbon chains are much more polar than the saturated ones. Thus, our new probes provided clear evidence that the polarity of LDs can be directly controlled by the length and unsaturation level of the fatty acids added to the cell diet.

Conclusions

In a search for new advanced environment-sensitive dyes, we developed two push-pull solvatochromic dyes based on naphthalene and fluorene core bearing an exceptionally strong electron acceptor, trifluoroacetyl group. The latter induced dramatic improvement in the optical properties of these dyes in comparison to their analogues with an aldehyde acceptor group: shift in their absorption and emission to the red, increase in their extinction coefficient, photostability, and sensitivity to solvent polarity (solvatochromism). These results indicated that boosting electron acceptor properties in the push-pull naphthalene and fluorene can lead to further enhancement in the excited state charge transfer character of the dyes. The obtained dyes ProCF3 and FrCF3 are among the smallest solvatochromic dyes operating in the visible spectrum, which exhibit even higher solvatochromism than the aldehyde analogue FR0, the reference compact solvatochromic dye to beat.^{1,39} In contrast to classical solvatochromic dyes, such as parent aldehydes and Nile Red, the new dyes exhibited strong fluorescence quenching by mM concentrations of water in organic solvents. This quenching could be explained by (a) high excited-state charge transfer character of these dyes, which could favor twisted intramolecular charge transfer (TICT)³⁰, and (b) addition of water to highly electrophilic carbonyl group, which breaks the conjugation of the dye. In live cells, the trifluoroacetyl dyes exhibited high specificity to LDs, showing remarkably low background in other cell compartments. In contrast, parent aldehydes and Nile Red showed detectable background from intracellular membranes. Experiments in model lipid membranes and nanoemulsion droplets confirmed high selectivity of new probes to LDs in contrast to classical solvatochromic dyes, which emit equally well in these two types

of lipid structures. Thus, strong fluorescence quenching of these dyes made them poorly emissive in lipid membranes, characterized by highly hydrated interface. Strong emission in LDs is clearly due to the presence of its oil core, where they are effectively shielded from bulk water. Therefore, ProCF₃ and FrCF₃ can be considered as the first-in-class solvatochromic probes for sensing the polarity of LDs oil core. Experiments in oils showed that their polarity response correlated with the length of fatty acid chains (shorter chains - higher polarity) and unsaturation levels (higher unsaturation – higher polarity). Their ratiometric imaging in cells revealed strong heterogeneity in polarity within LDs, which covered the range of polarities of unsaturated triglyceride oils. In contrast, Nile Red failed to properly estimate local polarity of LDs, producing imaging artefacts due to significant emission from intracellular membranes. Finally, ProCF₃ and FrCF₃ probes revealed that the polarity of LDs core can be altered by fatty acid diets. Thus, the increase in the unsaturation of fatty acids produced a significant increase in local LDs core polarity, whereas increases in the fatty chain length produced the opposite effect. The new probes will allow monitoring LDs core composition and properties and their evolution under different stress conditions. We expect ProCF₃ and FrCF₃ and their analogues will find applications in the studies of other natural and synthetic systems, presenting hydrophobic core, such as lipoproteins and synthetic lipidic and polymeric nanoparticles, etc. Moreover, the obtained results suggest trifluoroacetyl group is a powerful acceptor group in the design of advanced solvatochromic dyes.

Materials and methods

Synthesis

All the reagents were purchased from Sigma-Aldrich, Alfa Aesar, or TCI and used without any further purification. MilliQ-water (Millipore) was used in all relevant experiments. NMR spectra were recorded on a BrukerAvance III 400 MHz spectrometer. Mass spectra were obtained using an Agilent Q-TOF 6520 mass spectrometer with electrospray ionization (ESI). 7-bromo-N,N-diethyl-9,9-dimethyl-9H-fluoren-2-amine (compound **4**) and 7-(diethylamino)-9,9-dimethyl-9H-fluorene-2-carbaldehyde (FR0) were synthesized as described previously.³⁹ Synthesis of new dyes ProCF₃ and FrCF₃ is described in supporting information.

Spectroscopy

Absorption and emission spectra were recorded on an Agilent Cary 5000 UV–vis–NIR spectrophotometer and an Edinburgh FS5 spectrofluorometer, correspondingly. QYs were determined from the absorbance values at the excitation wavelength 380 nm for ProCF₃ and 400 nm for FrCF₃ and the integral over the whole emission range using a simplified relative method with PK in DCM (QY = 0.99)⁵³ as a standard.

Cell Lines, Culture Conditions, and Treatment

U87 (ATCC HTB-14) cells were grown in Dulbecco's modified eagle medium (EMEM, Gibco Invitrogen) and supplemented with 10% fetal bovine serum (FBS, Lonza), 1% L-glutamine (Sigma-Aldrich), 1% non-essential amino acid solution (Gibco-Invitrogen) and sodium pyruvate 1 mmol/L at 37 °C in a humidified 5% CO₂ atmosphere. Cells were seeded onto a chambered coverglass (IBIDI) at a density of 5×10^4 cells/well 24 h before the microscopy measurement. For microscopy imaging, the attached live cells in IBIDI dishes were washed once with warm phosphate-buffered saline (PBS).

After that, 1 mL of a corresponding dye solution in reduced serum medium (Opti-MEM, Gibco Invitrogen) was added and the cells were incubated for 10 min at room temperature before imaging.

Fluorescence Microscopy

Confocal imaging of cells and oils was performed on a Leica TCS SP8 confocal microscope with HCX PL APO 63×/ 1.40 OIL CS2 objective and two 12-bit photomultipliers. The excitation light was provided by lasers of 405 nm (50 mW at 100% power) for ProCF3, FrCF3 and 488 nm (20 mW at 100% power) for Nile Red. All the parameters at each channel were left constant; the illumination power was adjusted to achieve a good signal for each probe. The laser power settings were as follows: 5% of maximum intensity for each excitation. All the images were processed using ImageJ. Colocalization analysis was done using ImageJ macro (Colocalization Finder, developed by P. Carl, University of Strasbourg). Before the analysis, binning 2×2 was applied to all images (512×512 final image resolution) in order to improve signal-to-noise ratio. Four images were analyzed per condition and an average value of Pearson's coefficient was obtained in each case. Ratiometric confocal imaging was performed on a Leica TCS SP8 confocal microscope with HXC PL APO 63×/1.40 OIL CS2 objective. The wavelength range for individual channels are provided in corresponding figure legends. The ratiometric images were generated by using a special macro (RatioloJ, developed by R. Vauchelles, University of Strasbourg) under ImageJ that divides the image of one channel by the other. For each pixel, a pseudocolor scale was used for coding the ratio, while the intensity was defined by the integral intensity recorded for both channels at the corresponding pixel. Fatty acid diet was induced by incubating the cells with a solution of EMEM containing fatty acid in FA-free BSA for 24 h at 37 °C. The concentrations of fatty acids were the following: 200 μM for palmitic and oleic acid, 150 μM for linoleic acid, 100 μM for gondoic acid and 20 μM for DHA.

Supporting Information

Some experimental details; scheme of synthesis and NMR spectra for all compounds; additional experimental data, including absorption and fluorescence spectra and fluorescence microscopy images.

Acknowledgments

This work was supported by the Interdisciplinary Thematic Institute SysChem, via the IdEx Unistra (ANR-10-IDEX-0002), the CSC Graduate School (CSC-IGS ANR-17-EURE-0016) within the French Investments for the Future Program and Agence Nationale de la Recherche (ANR) AmpliSens ANR-21-CE42-0019-01 and SenEmul ANR-22-CE18-0034. Valeria Jose Boide-Trujillo is acknowledged for preparation of lipid nanoemulsions.

References

- (1) Klymchenko, A. S. Solvatochromic and Fluorogenic Dyes as Environment-Sensitive Probes: Design and Biological Applications. *Acc. Chem. Res.* **2017**, *50*, 366-375.
- (2) Reichardt, C. Solvatochromic Dyes as Solvent Polarity Indicators. *Chem. Rev.* **1994**, *94*, 2319-2358.
- (3) Klymchenko, A. S. Fluorescent Probes for Lipid Membranes: From the Cell Surface to Organelles. *Acc. Chem. Res.* **2023**, *56*, 1-12.

- (4) Kucherak, O. A.; Oncul, S.; Darwich, Z.; Yushchenko, D. A.; Arntz, Y.; Didier, P.; Mély, Y.; Klymchenko, A. S. Switchable Nile Red-Based Probe for Cholesterol and Lipid Order at the Outer Leaflet of Biomembranes. *J. Am. Chem. Soc.* **2010**, *132*, 4907-4916.
- (5) Dietrich, C.; Bagatolli, L. A.; Volovyk, Z. N.; Thompson, N. L.; Levi, M.; Jacobson, K.; Gratton, E. Lipid Rafts Reconstituted in Model Membranes. *Biophys. J.* **2001**, *80*, 1417-1428.
- (6) Jin, L.; Millard, A. C.; Wuskell, J. P.; Dong, X.; Wu, D.; Clark, H. A.; Loew, L. M. Characterization and Application of a New Optical Probe for Membrane Lipid Domains. *Biophys. J.* **2006**, *90*, 2563-2575.
- (7) Danylchuk, D. I.; Jouard, P. H.; Klymchenko, A. S. Targeted Solvatochromic Fluorescent Probes for Imaging Lipid Order in Organelles under Oxidative and Mechanical Stress. *J. Am. Chem. Soc.* **2021**, *143*, 912-924.
- (8) Vázquez, M. E.; Blanco, J. B.; Imperiali, B. Photophysics and Biological Applications of the Environment-Sensitive Fluorophore 6-N,N-Dimethylamino-2,3-Naphthalimide. *J. Am. Chem. Soc.* **2005**, *127*, 1300-1306.
- (9) Venkatraman, P.; Nguyen, T. T.; Sainlos, M.; Bilsel, O.; Chitta, S.; Imperiali, B.; Stern, L. J. Fluorogenic Probes for Monitoring Peptide Binding to Class II MHC Proteins in Living Cells. *Nat. Chem. Biol.* **2007**, *3*, 222-228.
- (10) Bongiovanni, M. N.; Godet, J.; Horrocks, M. H.; Tosatto, L.; Carr, A. R.; Wirthensohn, D. C.; Ranasinghe, R. T.; Lee, J.-E.; Ponjavic, A.; Fritz, J. V.; Dobson, C. M.; Klenerman, D.; Lee, S. F. Multi-Dimensional Super-Resolution Imaging Enables Surface Hydrophobicity Mapping. *Nat. Commun.* **2016**, *7*, 13544.
- (11) Moon, S.; Yan, R.; Kenny, S. J.; Shyu, Y.; Xiang, L.; Li, W.; Xu, K. Spectrally Resolved, Functional Super-Resolution Microscopy Reveals Nanoscale Compositional Heterogeneity in Live-Cell Membranes. *J. Am. Chem. Soc.* **2017**, *139*, 10944-10947.
- (12) Danylchuk, D. I.; Moon, S.; Xu, K.; Klymchenko, A. S. Switchable Solvatochromic Probes for Live-Cell Super-Resolution Imaging of Plasma Membrane Organization. *Angew. Chem. Int. Ed. Engl.* **2019**, *58*, 14920-14924.
- (13) Zhanghao, K.; Liu, W.; Li, M.; Wu, Z.; Wang, X.; Chen, X.; Shan, C.; Wang, H.; Chen, X.; Dai, Q.; Xi, P.; Jin, D. High-Dimensional Super-Resolution Imaging Reveals Heterogeneity and Dynamics of Subcellular Lipid Membranes. *Nat. Commun.* **2020**, *11*, 5890.
- (14) Jiménez-Sánchez, A.; Lei, E. K.; Kelley, S. O. A Multifunctional Chemical Probe for the Measurement of Local Micropolarity and Microviscosity in Mitochondria. *Angew. Chem. Int. Ed. Engl.* **2018**, *57*, 8891-8895.
- (15) Wang, K.; Ma, S.; Ma, Y.; Zhao, Y.; Xing, M.; Zhou, L.; Cao, D.; Lin, W. Aurone Derivative Revealing the Metabolism of Lipid Droplets and Monitoring Oxidative Stress in Living Cells. *Anal. Chem.* **2020**, *92*, 6631-6636.
- (16) He, D.; Yan, M.; Sun, Q.; Zhang, M.; Xia, Y.; Sun, Y.; Li, Z. Ketocyanine-Based Fluorescent Probe Revealing the Polarity Heterogeneity of Lipid Droplets and Enabling Accurate Diagnosis of Hepatocellular Carcinoma. *Adv. Healthc. Mater.* **2024**, *13*, 2303212.
- (17) Fan, L.; Wang, X.; Zan, Q.; Fan, L.; Li, F.; Yang, Y.; Zhang, C.; Shuang, S.; Dong, C. Lipid Droplet-Specific Fluorescent Probe for in Vivo Visualization of Polarity in Fatty Liver, Inflammation, and Cancer Models. *Anal. Chem.* **2021**, *93*, 8019-8026.
- (18) Sha, J.; Liu, W.; Zheng, X.; Guo, Y.; Li, X.; Ren, H.; Qin, Y.; Wu, J.; Zhang, W.; Lee, C.-S.; Wang, P. Polarity-Sensitive Probe for Two-Photon Fluorescence Lifetime Imaging of Lipid Droplets in Vitro and in Vivo. *Anal. Chem.* **2023**, *95*, 15350-15356.
- (19) Fam, T. K.; Klymchenko, A. S.; Collot, M. Recent Advances in Fluorescent Probes for Lipid Droplets. *Materials (Basel)* **2018**, *11*.
- (20) Collot, M.; Bou, S.; Fam, T. K.; Richert, L.; Mély, Y.; Danglot, L.; Klymchenko, A. S. Probing Polarity and Heterogeneity of Lipid Droplets in Live Cells Using a Push-Pull Fluorophore. *Anal. Chem.* **2019**, *91*, 1928-1935.
- (21) Ashoka, A. H.; Ashokkumar, P.; Kovtun, Y. P.; Klymchenko, A. S. Solvatochromic near-Infrared Probe for Polarity Mapping of Biomembranes and Lipid Droplets in Cells under Stress. *J. Phys. Chem. Lett.* **2019**, *10*, 2414-2421.
- (22) Shyu, P., Jr.; Wong, X. F. A.; Crasta, K.; Thibault, G. Dropping in on Lipid Droplets: Insights into Cellular Stress and Cancer. *Biosci. Rep.* **2018**, *38*, BSR20180764.
- (23) Martin, S.; Parton, R. G. Lipid Droplets: A Unified View of a Dynamic Organelle. *Nat. Rev. Mol. Cell Biol.* **2006**, *7*, 373-378.

- (24) Farese, R. V., Jr.; Walther, T. C. Lipid Droplets Finally Get a Little R-E-S-P-E-C-T. *Cell* **2009**, *139*, 855-860.
- (25) Zadoorian, A.; Du, X. M.; Yang, H. Y. Lipid Droplet Biogenesis and Functions in Health and Disease. *Nat. Rev. Endocrinol.* **2023**, *19*, 443-459.
- (26) Filali-Mouncef, Y.; Hunter, C.; Roccio, F.; Zagkou, S.; Dupont, N.; Primard, C.; Proikas-Cezanne, T.; Reggiori, F. The Menage a Trois of Autophagy, Lipid Droplets and Liver Disease. *Autophagy* **2022**, *18*, 50-72.
- (27) Krahmer, N.; Farese, R. V.; Walther, T. C. Balancing the Fat: Lipid Droplets and Human Disease. *EMBO Mol. Med.* **2013**, *5*, 973-983.
- (28) Greenberg, A. S.; Coleman, R. A.; Kraemer, F. B.; McManaman, J. L.; Obin, M. S.; Puri, V.; Yan, Q. W.; Miyoshi, H.; Mashek, D. G. The Role of Lipid Droplets in Metabolic Disease in Rodents and Humans. *J. Clin. Invest.* **2011**, *121*, 2102-2110.
- (29) Niko, Y.; Didier, P.; Mely, Y.; Konishi, G.-i.; Klymchenko, A. S. Bright and Photostable Push-Pull Pyrene Dye Visualizes Lipid Order Variation between Plasma and Intracellular Membranes. *Sci. Rep.* **2016**, *6*, 18870.
- (30) Grabowski, Z. R.; Rotkiewicz, K.; Rettig, W. Structural Changes Accompanying Intramolecular Electron Transfer: Focus on Twisted Intramolecular Charge-Transfer States and Structures. *Chem. Rev.* **2003**, *103*, 3899-4032.
- (31) Hansch, C.; Leo, A.; Taft, R. W. A Survey of Hammett Substituent Constants and Resonance and Field Parameters. *Chem. Rev.* **1991**, *91*, 165-195.
- (32) Kim, D.-S.; Ahn, K. H. Fluorescence "Turn-on" Sensing of Carboxylate Anions with Oligothiophene-Based O-(Carboxamido)Trifluoroacetophenones. *J. Org. Chem.* **2008**, *73*, 6831-6834.
- (33) Mohr, G. J. New Chromoreactants for the Detection of Aldehydes, Amines and Alcohols. *Sens. Actuators B Chem.* **2003**, *90*, 31-36.
- (34) Mohr, G. J.; Lehmann, F.; Grummt, U.-W.; Spichiger-Keller, U. E. Fluorescent Ligands for Optical Sensing of Alcohols: Synthesis and Characterisation of P-N,N-Dialkylamino-Trifluoroacetylstilbenes. *Anal. Chim. Acta* **1997**, *344*, 215-225.
- (35) Xu, Y.; Yu, S.; Wang, Y.; Hu, L.; Zhao, F.; Chen, X.; Li, Y.; Yu, X.; Pu, L. Ratiometric Fluorescence Sensors for 1,2-Diamines Based on Trifluoromethyl Ketones. *European J. Org. Chem.* **2016**, *2016*, 5868-5875.
- (36) García-Calvo, J.; Maillard, J.; Fureraj, I.; Strakova, K.; Colom, A.; Mercier, V.; Roux, A.; Vauthey, E.; Sakai, N.; Fürstenberg, A.; Matile, S. Fluorescent Membrane Tension Probes for Super-Resolution Microscopy: Combining Mechanosensitive Cascade Switching with Dynamic-Covalent Ketone Chemistry. *J. Am. Chem. Soc.* **2020**, *142*, 12034-12038.
- (37) Chen, X.-X.; Bayard, F.; Gonzalez-Sanchis, N.; Pamungkas, K. K. P.; Sakai, N.; Matile, S. Fluorescent Flippers: Small-Molecule Probes to Image Membrane Tension in Living Systems. *Angew. Chem. Int. Ed. Engl.* **2023**, *62*, e202217868.
- (38) Weber, G.; Farris, F. J. Synthesis and Spectral Properties of a Hydrophobic Fluorescent Probe: 6-Propionyl-2-(Dimethylamino)Naphthalene. *Biochemistry* **1979**, *18*, 3075-3078.
- (39) Kucherak, O. A.; Didier, P.; Mély, Y.; Klymchenko, A. S. Fluorene Analogues of Prodan with Superior Fluorescence Brightness and Solvatochromism. *J. Phys. Chem. Lett.* **2010**, *1*, 616-620.
- (40) Kucherak, O. A.; Richert, L.; Mély, Y.; Klymchenko, A. S. Dipolar 3-Methoxychromones as Bright and Highly Solvatochromic Fluorescent Dyes. *Phys. Chem. Chem. Phys.* **2012**, *14*, 2292-2300.
- (41) Niko, Y.; Kawauchi, S.; Konishi, G.-i. Solvatochromic Pyrene Analogues of Prodan Exhibiting Extremely High Fluorescence Quantum Yields in Apolar and Polar Solvents. *Chem. Eur. J.* **2013**, *19*, 9760-9765.
- (42) Wang, H.; Zhang, C.; Hu, L.; Tang, F.; Wang, Y.; Ding, F.; Lu, J.; Ding, A. Red-Emissive Dual-State Fluorogenic Probe for Wash-Free Imaging of Lipid Droplets in Living Cells and Fatty Liver Tissues. *Chem. Asian J.* **2023**, *18*, e202201291.
- (43) Ho, C.; Slater, S. J.; Stubbs, C. D. Hydration and Order in Lipid Bilayers. *Biochemistry* **1995**, *34*, 6188-6195.
- (44) Klymchenko, A. S.; Mély, Y.; Demchenko, A. P.; Duportail, G. Simultaneous Probing of Hydration and Polarity of Lipid Bilayers with 3-Hydroxyflavone Fluorescent Dyes. *Biochim. Biophys. Acta* **2004**, *1665*, 6-19.
- (45) Bagatolli, L. A.; Gratton, E.; Fidelio, G. D. Water Dynamics in Glycosphingolipid Aggregates Studied by Laurdan Fluorescence. *Biophys. J.* **1998**, *75*, 331-341.
- (46) Klymchenko, A. S.; Liu, F.; Collot, M.; Anton, N. Dye-Loaded Nanoemulsions: Biomimetic Fluorescent Nanocarriers for Bioimaging and Nanomedicine. *Adv. Healthc. Mater.* **2021**, *10*, e2001289.

- (47) Anton, N.; Vandamme, T. F. Nano-Emulsions and Micro-Emulsions: Clarifications of the Critical Differences. *Pharm. Res.* **2011**, *28*, 978-985.
- (48) de la Rosa Rodriguez, M. A.; Deng, L.; Gemmink, A.; van Weeghel, M.; Aoun, M. L.; Warnecke, C.; Singh, R.; Borst, J. W.; Kersten, S. Hypoxia-Inducible Lipid Droplet-Associated Induces Dgat1 and Promotes Lipid Storage in Hepatocytes. *Mol. Metab.* **2021**, *47*, 101168.
- (49) Eynaudi, A.; Díaz-Castro, F.; Bórquez, J. C.; Bravo-Sagua, R.; Parra, V.; Troncoso, R. Differential Effects of Oleic and Palmitic Acids on Lipid Droplet-Mitochondria Interaction in the Hepatic Cell Line Hepg2. *Front Nutr* **2021**, *8*, 775382.
- (50) Pawlak, P.; Malyszka, N.; Szczerbal, I.; Kolodziejcki, P. Fatty Acid Induced Lipolysis Influences Embryo Development, Gene Expression and Lipid Droplet Formation in the Porcine Cumulus Cells†. *Biol. Reprod.* **2020**, *103*, 36-48.
- (51) Danielli, M.; Perne, L.; Jarc Jovičić, E.; Petan, T. Lipid Droplets and Polyunsaturated Fatty Acid Trafficking: Balancing Life and Death. *Front. Cell. Dev. Biol.* **2023**, *11*, 1104725.
- (52) Plötz, T.; Hartmann, M.; Lenzen, S.; Elsner, M. The Role of Lipid Droplet Formation in the Protection of Unsaturated Fatty Acids against Palmitic Acid Induced Lipotoxicity to Rat Insulin-Producing Cells. *Nutr. Metab. (Lond.)* **2016**, *13*, 16.
- (53) Valanciunaite, J.; Kempf, E.; Seki, H.; Danylchuk, D. I.; Peyriéras, N.; Niko, Y.; Klymchenko, A. S. Polarity Mapping of Cells and Embryos by Improved Fluorescent Solvatochromic Pyrene Probe. *Anal. Chem.* **2020**, *92*, 6512-6520.

TOC graphic

